

# Fatigue cracking prediction of cobblestone interlayer pavement using non-destructive testing and mechanistic-empirical analyses

*Previsão de fissuração por fadiga em pavimentos intercalares de paralelepípedos usando ensaios não destrutivos e análises mecanicista-empíricas*

Giovanni Pasquale Beninca<sup>1</sup>, Adriana Goulart dos Santos<sup>1</sup>

<sup>1</sup>Universidade do Estado de Santa Catarina, Joinville, Santa Catarina, Brasil

Contact: giovannibeninca@outlook.com,  (GPB), adriana.santos@udesc.br,  (AGS)

## Submitted:

10 June, 2024

## Revised:

25 July, 2024

## Accepted for publication:

31 August, 2024

## Published:

30 October 2024

## Associate Editor:

Francisco Thiago Sacramento Aragão,  
Universidade Federal do Rio de  
Janeiro, Brasil

## Keywords:

Backcalculation.  
FWD.  
Cobblestone.  
Fatigue cracking.  
MeDiNa.

## Palavras-chave:

Retroanálise.  
FWD.  
Paralelepípedo.  
Fissuração por fadiga.  
MeDiNa.

DOI: 10.58922/transportes.v32i3.3022

## ABSTRACT

Several non-destructive testing (NTD) methods have been used to measure surface deflection, which makes to determine the elastic moduli of pavement layers through the back-calculation process and assess the structural capacity of asphalt pavements. In this study was evaluated the back-calculated moduli of the cobblestone interlayer pavements and the load capacity of this type of pavement related to the fatigue cracking criterion based on a mechanistic-empirical analysis. The employed methodology included the performance of on-site trials using non-destructive testing with the Falling Weight Deflectometer (FWD) devices on 84 test points in granular and cobblestone interlayer pavements, determination of deflection basin parameters (DBP), back-calculation layers' moduli, and estimate of the fatigue cracking performance of the pavements by mechanistic-empirical analyses in MeDiNa software. The pavements with a cobblestone base layer displayed greater deflection measurements on the load application point compared to those measured on pavements with a granular base layer, indicating that conventional pavement displayed more stiffness. Cobblestone interlayer pavement displayed greater amounts of cracked area compared to granular base layer pavements showing lower load capacity based on the fatigue criterion. The DBP-based method by FWD test was able to identify the structural differences between the layers of pavements evaluated and identify the cracking evolution.

## RESUMO

Vários métodos de ensaios não destrutivos (END) têm sido utilizados para medir a deflexão superficial, o que permite determinar os módulos elásticos das camadas do pavimento através do processo de retroanálise e avaliar a capacidade estrutural dos pavimentos asfálticos. Neste estudo, foram avaliados os módulos retroanalizados de pavimentos intercalados de paralelepípedos e a capacidade de carga deste tipo de pavimento relacionada ao critério de fissuração por fadiga com base em uma análise mecanística-empírica. A metodologia empregada incluiu a realização de ensaios in situ utilizando END com equipamento Falling Weight Deflectometer (FWD) em 84 pontos de ensaio em pavimentos construídos tanto em base granular como em paralelepípedos, determinação de parâmetros de bacia de deflexão (DBP), retroanálise dos módulos das camadas e estimativa de desempenho por fissuração por fadiga por meio de análises mecanística-empíricas no software MeDiNa. Os pavimentos com camada de base de paralelepípedos apresentaram maiores medidas de deflexão no ponto de aplicação da carga em comparação com aquelas medidas em pavimentos com camada de base granular, indicando que este tipo de pavimento apresentou maior rigidez. Pavimentos com base em paralelepípedo apresentaram maior quantidade de área fissurada em comparação ao pavimento com base granular, apresentando menor capacidade de carga no tocante ao critério de fadiga. Foi evidenciado que o método baseado em DBP determinados pelas bacias medidas pelo teste FWD foi capaz de identificar as diferenças estruturais entre as camadas dos pavimentos avaliados, bem como a identificação da evolução de suas fissurações.



## 1. INTRODUCTION

In recent years most cobblestone pavements in urban areas have been replaced or converted into traditional flexible pavement, covered with overlaid concrete asphalt mixtures (Garilli et al., 2020). This type of pavement relies on the stress state of the unbound stone interlayer to withstand the traffic loads, which typically affects a relatively larger pavement area (Autelitano et al., 2020).

The performances of pavements are greatly affected by the heterogeneity of material and structure composition, and their mechanical responses vary greatly under different load conditions. So, the pavement structural evaluation is of great importance to design, construction and management (Jiang et al., 2020).

By analyzing the structural capacity of pavements, agencies can track their behavior over time and consequently define optimal intervention times to maximize performance. Structural information also allows the optimization of design construction processes through increased knowledge of pavement deterioration trends (Camacho-Garita et al., 2019). Pavement structural evaluation consists of calculating its load capacity. It is obtained based on various parameters, such as deflection, which makes to determine the elastic moduli of pavement layers through the back-calculation process (Mabrouk et al., 2020).

The back-calculated layer moduli are then used to compute the pavement response under vehicle loading and evaluate the pavement performance. The process of back-calculation searches for the solution of the inverse problem obtained by calculating the deflected shape of a pavement structure, as a function of the thickness of the pavement layers, the moduli of individual layers and the magnitude of the load (Scimemi et al., 2016).

Several non-destructive testing (NTD) methods have been used to measure surface deflection and assess the structural capacity of asphalt pavements, such as the light weight deflectometer, benkelman beam, heavy weight deflectometer and falling weight deflectometer. The falling weight deflectometer (FWD) is one of the most useful and popular techniques used to evaluate the pavement structural capacity among all NDT methods (Kheradmandi and Modarres, 2018). FWD is an impulse loading device whereby the transient load is applied to the pavement, and the surface's deflection shape is measured (Singh et al., 2020). Due to several advantages, such as the short testing duration, the application of different load levels with high accuracy and low dispersion in measured deflections (Pais et al., 2020), FWD devices are currently used to obtain the elastic moduli of each pavement layer by analyzing pavement surface deflections, based on back-calculation (Sangghaleh et al. 2014).

During the mechanistic-empirical (M-E) pavement design and analysis process, the mechanical responses of a pavement layer, such as stress, strain, and deflection, are important indexes to characterize the loading state of pavement, which are often used to evaluate the ability to resist cracks, deformation, and other pavement diseases (Qian et al., 2021). Mechanistic-Empirical Pavement Design utilizes the theory of elastic analysis to calculate strains at critical locations that may result in the failure of the pavement structure (El-Ashwah et al., 2021).

Fatigue cracking (FC) is one of the most critical types of failure in flexible pavements subjected to repeated applied wheel loads. Applied vehicular load induces micro-cracks as each application eventually causes macro-cracks and failure (Gong et al., 2017). In the M-E pavement design, the FC, represented in percent of lane area, is associated with the critical mechanical responses through an empirical mathematical model called the Transfer Function (FT) (Gong et al., 2017). The TF correlates the critical mechanistic responses, such as the stress and strain to observable field performance through an empirical statistical equation (AASHTO, 2015).

Previous studies have proposed to use advance laboratory testing (Oteki et al., 2024; Zhang et al., 2023; Yang et al., 2023; Ishaq and Giustozzi, 2021) and numerical modeling (Wang and An, 2024; Zhao and Wang, 2021; Norouzi et al., 2022) to evaluate fatigue life models of asphalt mixtures and calculate critical pavement responses responsible for fatigue cracking of asphalt pavements. However, the fatigue cracking behavior of pavements subjected to an impact of dynamic loads deflector for effective performance and life prediction has not been considered in the framework of M-E pavement design and analysis.

In this context, there have been few studies on the effectiveness of utilizing FWD to evaluate the structural conditions of stone interlayer pavements. Titi et al. (2003) investigated the long-term performance of the stone interlayer pavement subjected to an accelerated loading system. The results showed that the stone interlayer pavement design experienced less cracking density compared to the conventional design after 10.2 years of service. Chen et al. (2014) studied the field performance of a test section of stone interlayer pavement and cement-stabilized base test control section on LA-97 in Acadia Parish, Louisiana. After about 20 years of service, the stone interlayer had a cracking density of 34.7%, while the control section had a cracking density of 56.3%. Also, the cracking severity levels of the control section were higher than those of the stone interlayer section. However, no study evaluates the structural conditions of stone interlayers in urban pavements.

The objective of this study is to evaluate the elastic moduli of the cobblestone interlayer pavements, back-calculated from FWD trial, and estimate the traffic loading capability of this type of pavement subjected to the fatigue cracking criterion using mechanistic-empirical (ME) analyses. It is important to investigate the fatigue cracking behavior of cobblestones interlayer pavements when subjected to an impact load of an FWD deflector for effective performance and life prediction. For the flexible pavement with cobblestone base layer, the comprehensive performance evaluation of the in-service pavement must include structural performance, not only concrete asphalt layer but also base layer.

## 2. FATIGUE CRACKING PREDICTION

Over the years, many researchers have attempted to study fatigue characteristics and develop mathematical models to predict asphalt mixture fatigue life. There are two main approaches to characterizing material fatigue behavior in the laboratory: mechanistic and phenomenological approaches.

The mechanistic approach accounts for how the damage evolves throughout the fatigue life at different loads and environmental conditions, leading to a better estimation of the fatigue behavior of asphalt mixtures (Klug et al., 2022). In this approach, the Viscoelastic Continuum Damage (VECD) theory for the fatigue prediction model has been applied as a modern method to estimate the mechanical behavior of asphalt mixtures (Underwood et al., 2012; Sabouri and Kim, 2014; Cao et al., 2018; Wang et al., 2020).

The phenomenological models relate the stress or strain in the specimen to the number of failure cycles (Babadopulos et al., 2015; Saboo et al., 2016; Delgadillo and Monsalve, 2021; Wang et al., 2018). These strains are then related to pavement life using various fatigue equations as transfer functions (TF) according to the mechanistic-empirical pavement design method. Those functions translate into how the laboratory test “accelerates” the fatigue phenomenon related to field performance. They estimate the service life of a proposed pavement structure using the results from Whöler curves and pavement elastic analysis (Babadopulos et al., 2015). The prediction precision of the empirical models depends heavily on the design parameters’ hierarchical input levels and the transfer functions’ calibration.

Brazil developed its method for a mechanistic-empirical asphalt pavement design for this purpose based on a national pavement material database and the performance of test sections monitored throughout the country. The “Método de Dimensionamento Nacional” (MeDiNa) addresses the mechanistic-empirical methodology for designing the implementation and rehabilitation analyses of pavements.

In the MeDiNa software, a Transfer Function (TF) receives data on the average damage and reduced average damage arising from structural analysis and other adopted premises and informs the percentage of the cracked area (CA%) for that situation of estimated average damage (Franco, 2007). The current TF was calibrated by the research studies performed by Fritzen et al. (2019). This study utilizes the MeDiNa software to perform the evaluated pavements’ empirical mechanistic analyses.

## 2.1. Fatigue damage

The MeDiNa manual points out that the software uses the calculated stress state at ten points on the top of asphalt concrete layer, in 3.65 cm spaced intervals, and at ten points on the bottom of the asphalt concrete layer. Hence, fatigue damage is determined in each of these twenty points to calculate the average. Based on that average, the program calculates the cracked area using the transfer function as defined by Fritzen et al. (2019).

The fatigue curve adopted in MeDiNa is obtained by the diametral compression tests. As indicated in the MeDiNa Manual, the software only allows cycle number to failure ( $N_{fad}$ ) relationships with the resilient strain deformation ( $\varepsilon_t$ ), as stated in Equation 1, where  $k_1$  and  $k_2$  are factors related to the quality of the materials.

$$N_{fad} = k_1 \varepsilon_t^{k_2} \quad (1)$$

where:  $N_{fad}$  = number of cycles;  $\varepsilon_t$  = specific resilient strain deformation;  $k_1$  and  $k_2$  = fatigue curve parameters.

## 3. RESEARCH METHODOLOGY

The employed methodology included the performance of on-site trials using the FWD devices on 84 test points, determination of deflection basin parameters (DBP), back-calculation layers’ moduli, and the estimate of the fatigue cracking performance of the pavements using mechanistic-empirical analyses. The performance of the cobblestone interlayer pavement was compared to the conventional pavement designed with well-compacted granular base and subbase layers. The DBP were used to evaluate the individual structural conditions of each layer of the conventional and cobblestone interlayer pavements.

### 3.1. Characterization of the evaluated pavements

Thirteen urban pavement segments were selected in the municipality of Balneário Camboriú, Santa Catarina, Brazil. Ten of the thirteen analyzed segments refer to urban roads where asphalt concrete layer was applied over a granite cobblestones layer, and three urban roads refer to conventional pavement designed with asphalt concrete layer over unbound granular base and subbase layers. These last three segments were selected to compare the obtained results between the two types of pavements (cobblestone interlayer and conventional). Table 1 displays the street names, the type of material of base layer, the year of their construction, the length of each segment, and the

number of test points measured by FWD device. For segments shorter than 100.00 meters, three test points were considered, with one being the central point of the segment and the other two equidistant from this point. For segments longer than 100.00 meters, test points were considered every 50.00 meters of track.

**Table 1:** Characterization of the analyzed pavement segments.

| Segment | Base Layer Type | Year Paved | Length (m) | Number of test points (FWD) |
|---------|-----------------|------------|------------|-----------------------------|
| 1       | Cobblestone     | 2018       | 042.00     | 3                           |
| 2       | Cobblestone     | 2020       | 167.50     | 4                           |
| 3       | Cobblestone     | 2017       | 200.50     | 4                           |
| 4       | Cobblestone     | 2020       | 180.00     | 4                           |
| 5       | Cobblestone     | 2020       | 270.00     | 6                           |
| 6       | Cobblestone     | 2020       | 330.00     | 7                           |
| 7       | Cobblestone     | 2020       | 335.00     | 7                           |
| 8       | Cobblestone     | 2020       | 366.50     | 7                           |
| 9       | Cobblestone     | 2020       | 323.50     | 6                           |
| 10      | Cobblestone     | 2020       | 235.00     | 4                           |
| 11      | Granular        | 2018       | 525.00     | 10                          |
| 12      | Granular        | 2019/2020  | 530.00     | 11                          |
| 13      | Granular        | 2019/2020  | 572.50     | 11                          |
| Total   |                 |            | 4077.50    | 84                          |

All the analyzed stone interlayer pavements had the same cross-section represented in Figure 1a, as follows: 7-cm thickness asphalt concrete (AC) on surface layer, 15-cm thickness granite cobblestones in base layer, 20-cm thickness sand bedding in subbase layer and gravel mixture constituted the subgrade layer. The shape of cobblestone elements is cubic with thickness of 15-cm. Natural sand was used as the jointing material. This pavement type is denoted herein as a cobblestone interlayer pavement.

Conventional pavements were constructed with base and subbase layers made of unbound granular materials. The cross-section of this pavement and the materials adopted in this project can be viewed in Figure 1b, as follows: 8-cm thickness asphalt concrete (AC) on surface layer, 15-cm thickness graded stone aggregate in base layer, 20-cm thickness crushed limestone in subbase layer and gravel mixture constituted the subgrade layer.

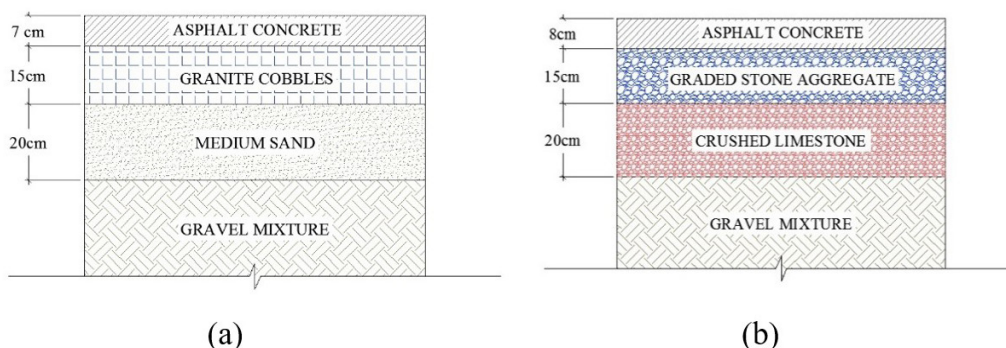


**Figure 1.** (a) Stone interlayer pavement profile; (b) Conventional pavement profile.



### 3.2. Performing deflectometric measurements using FWD device

KUAB 50 equipment (a Swedish brand) was equipped with a 30 cm diameter transfer plate for loading and seven deflection reading geophones positioned at distances of 0, 20, 30, 45, 60, 90, and 120 cm from the load center applied to the pavement. The FWD test was performed at an atmospheric temperature ranging from 17 °C to 27 °C and a pavement temperature from 25 °C to 34 °C. The temperature of the pavement surface and atmospheric were obtained using a meter of the equipment itself. The trials complied with the DNER-PRO 273 (1996), with a load applied to the pavement at approximately 40kN, and were carried out in March 2021. Figure 2a demonstrates the FWD device used in this study and Figure 2b demonstrates the positioning of the geophones.



(a)

(b)

Figure 2. (a) FWD KUAB device; (b) the positioning of the geophones.

### 3.3. Deflection basin parameters (DBP)

The DBP are powerful tools for a comprehensive analysis of the FWD data. In general, the DBP' values are obtained to facilitate structural analysis, and to provide a better understanding of the pavement behavior (Andrade et al., 2024). The DBP were calculated to evaluate the individual structural conditions of pavement layers; they are as follows: curvature radius (R), Superficial Curvature Index (SCI – this is the parameter that characterizes the structural behavior of the upper pavement layers, as they display greater sensitivity to temperature variation as the asphalt concrete displays thermosusceptible behavior), the Base Damage Index (BDI – an indicator of the structural condition of base and subbase layers) and the Base Curvature Index (BCI – an indicator of the subgrade structural condition).

Horak's method (Horak, 2008) was used in this study, which studied the effectiveness of deflection basin parameters in evaluating the structural condition of in-service pavements in South Africa. The basin parameters presented by Horak (2008) are more severe when compared to the study of Souza Jr. (2018) and Rocha (2020). Table 2 lists different DBP and corresponding threshold values as used by Horak (2008) in South Africa.

**Table 2:** Different DBP and corresponding threshold values.

| Performance Indicator | $D_0$ (0.01 mm) | $R$ (m) | SCI (0.01 mm) | BDI (0,01 mm) | BCI (0.01 mm) |
|-----------------------|-----------------|---------|---------------|---------------|---------------|
| Sound                 | <50             | >100    | <20           | <10           | <5            |
| Warning               | 50-75           | 50-100  | 20-40         | 10-20         | 5-10          |
| Severe                | >75             | <50     | >40           | >20           | >10           |

The mathematical expressions stated in Equations 2, 3, 4, and 5 were used to calculate these DBP. To obtain the curvature radius is necessary for interpolating the measured deflectometric values from point  $D_{20}$  to point  $D_{30}$  to obtain the deflection value  $D_{25}$ .

$$R = \frac{6250}{2 * (D_0 - D_{25})} \quad (2)$$

$$SCI = D_{30} - D_0 \quad (3)$$

$$BDI = D_{60} - D_{30} \quad (4)$$

$$BCI = D_{90} - D_{60} \quad (5)$$

where:  $D_0$ : the deflection point from the applied load [ $\times 10^{-2}$  mm]; and  $D_i$ : the deflection from  $i$  cm load application point [ $\times 10^{-2}$  mm].

### 3.4. Back-calculation

Back-calculation was performed by the BackMeDiNa software, version 1.2.0, which makes it possible to back-calculate moduli of the pavement layers based on the deflectometric basins obtained from the field by performing the FWD test. A total of eighty-four back-calculations were performed.

The following data were imported into the BackMeDiNa software: deflections, atmospheric and asphalt pavement temperatures and applied load. Subsequently, the materials and pavement layer thicknesses were informed. Poisson's ratios were determined according to the values pre-established by BackMeDiNa: 0.30 for the asphalt layers, 0.40 for the granular layers and 0.45 for the subgrade layer.

The initial values for the elastic moduli were stipulated, and the non-bonding interface condition between the layers was informed, considering the predefined conditions indicated in the MeDiNa method user's manual. The same initial values were used for the moduli as considered by Nery and Santos (2021), as 4000 MPa for the asphalt concrete layer, 300 MPa for the base layer (for unbound granular materials as well as for the stone), 200 MPa for the subbase layer, and 100 MPa for the subgrade layer.

### 3.5. Fatigue cracking prediction

The MeDiNa software was used (version v.1.1.5.0 - December/2020) to perform the mechanistic-empirical evaluation to estimate the performance of pavements analyzed by the fatigue rupture

criterion. The software considers 30% of the cracked area as the rupture criterion of the pavement over the project period, which was considered as 10 years. In this analysis, the average back-calculated moduli for each layer of the evaluated pavement were used.

The cracking percentage was verified in the 13 segments considering five hypothetical classes of traffic, considering the  $N_{AASHTO}$  number equal to  $10^5$  (light traffic),  $5 \times 10^5$  (medium traffic),  $2 \times 10^6$  (heavier traffic),  $2 \times 10^7$  (heavy traffic), and  $5 \times 10^7$  (very heavy traffic) for the equivalent standard axle load (80 kN), practiced in the IP-02 (2004) of the São Paulo City Hall, which classifies urban roads that will be designed, based on their expected traffic. Hence, it was possible to verify the traffic loading (N number) that the analyzed pavement can bear until it reaches its failure.

The fatigue curve for class 1 asphalt concrete mixture was used in this study, according pre-established asphalt mixtures in the software (Franco and Motta, 2018). Class 1 serves the project traffic's up to  $6 \times 10^6$  and the asphalt mixture moduli of 5,764 MPa. Equation 1 fatigue curve parameters are equal to:  $k_1 = 5,496.10^{-11}$  and  $k_2 = -3,253$ .

## 4. RESULTS AND DISCUSSIONS

### 4.1. Deflectometric evaluation

The thirteen analyzed segments were confirmed to be free of superficial cracking when examined by visual inspection during the FWD tests. Based on the graphic boxplot displayed in Figure 3, the descriptive statistic of the deflection measured at the point of load application (D0) can be analyzed for each evaluated segment. No outliers were found for the deflection measurements analyzed. Segments 1 to 10 refer to the stone interlayer pavements, and segments 11 to 13 refer to the conventional pavements.

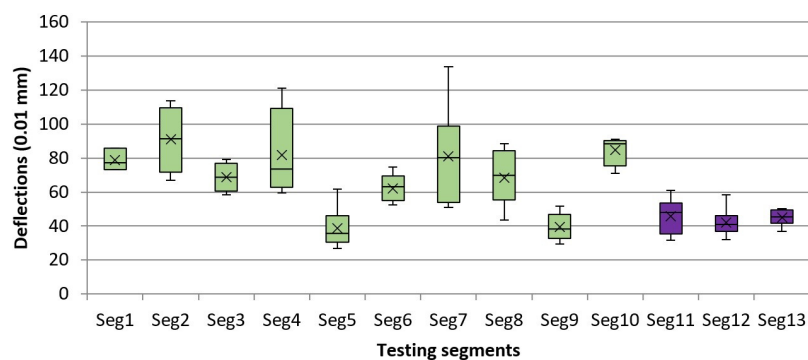


**Figure 3.** Descriptive statistic on deflection measurements at the load application point (D0) in each tested segment.

Analyzing Figure 3, the overall average of the deflection measurements in the segments with the cobblestone base layer was  $67.2 (\times 10^{-2} \text{ mm})$ , as the minimum value was equal to  $38.76 (\times 10^{-2} \text{ mm})$  in segment 5, and the maximum value was equal to  $90.92 (\times 10^{-2} \text{ mm})$  in segment 2. In the segments with the granular base layer, the overall average of the deflection measurements was  $44.3 (\times 10^{-2} \text{ mm})$ , as the minimum value was equal to  $41.94 (\times 10^{-2} \text{ mm})$  in segment 11 and the maximum value was equal to  $45.12 (\times 10^{-2} \text{ mm})$  in segment 10. This is indicating that the conventional pavement displayed more stiffness. In the studies by Chen et al. (2014, 2018), pavements with a stone base layer also presented greater deflection value measurements by the FWD device at



the load application point when compared with the measurements of deflection in the unbound granular base layer.

The average standard deviation of the measured deflections in the cobblestone interlayer pavements was  $23.66 (\times 10^{-2} \text{ mm})$ , with a minimum value of  $6.36 (\times 10^{-2} \text{ mm})$  in segment 1 and a maximum value of  $30.76 (\times 10^{-2} \text{ mm})$  in segment 7. In the conventional pavements, the standard measured deviation was  $7.51 (\times 10^{-2} \text{ mm})$ , with the minimum value as  $4.23 (\times 10^{-2} \text{ mm})$  in segment 13 and the maximum value as  $10.51 (\times 10^{-2} \text{ mm})$  in segment 11.

The average coefficient of variation (CV) for the cobblestone interlayer pavements was 35.23%, as the minimum value was equal to 8.08% in segment 1 and the maximum value was equal to 37.96% in segment 7. In the conventional pavements, the average CV was 16.97%, as the minimum value was 9.36% in segment 13 and the maximum value was 22.89% in segment 11. The Project Guideline IP-DE-P00/003 (DER, 2006) defines that the variation coefficients must be less than 30% to categorize a segment as homogeneous. The FWD trial achieved CV results of over 30% in three of the thirteen analyzed segments (segments 4, 5, and 7).

## 4.2. Deflection basin parameters (DBP)

Figure 4 displays the calculated average values of deflection basin parameters for each segment. All the curvature radius (R) values were about 100 meters or more, indicating good structural quality of the pavement. Most of the cobblestone interlayer pavements extrapolated the reference value of the SCI (Surface Curvature Index), indicating that the asphalt concrete layer is less resistant, and hence, it is more deformable.

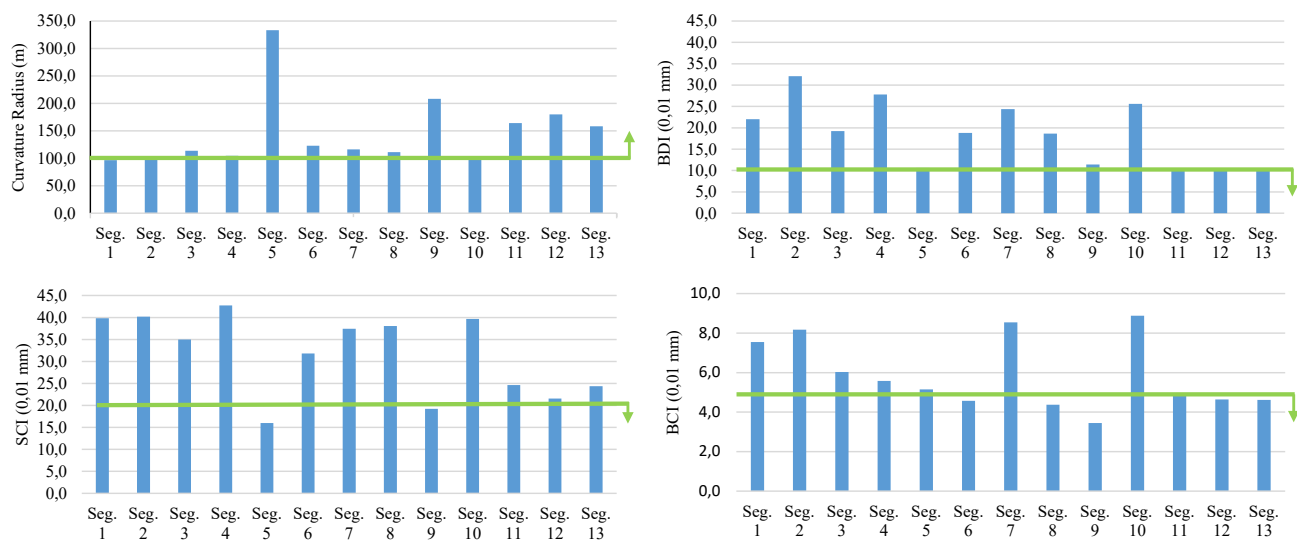


Figure 4. Deflection basin parameters. The green arrow represent limit values according to Horak (2008).

It is possible to confirm the parameters obtained from the conventional pavements were more homogenous and closer to the reference values than those related to stone interlayer pavements, as displayed in Figure 4. That can be justified due to employing technological control in the preparation of projects and the execution of conventional pavements, which does not apply to pavements made from stone interlayer pavements.

### 4.3. Comparison between back-calculated elastic moduli

The graph in Figure 5 displays the back-calculated elastic moduli for each of the 13 tested segments. The average back-calculated moduli of the asphalt concrete layer, in all the segments, were higher than the moduli of the other layers. In segments 1, 3, 6, 8, and 9, the subbase layer moduli of the cobblestone interlayer pavement were higher than the base layer moduli. In the three segments with granular base layers, the subbase layer moduli were higher than the base layer moduli. The subgrade layer achieved lower back-calculated moduli, except for segment 04.

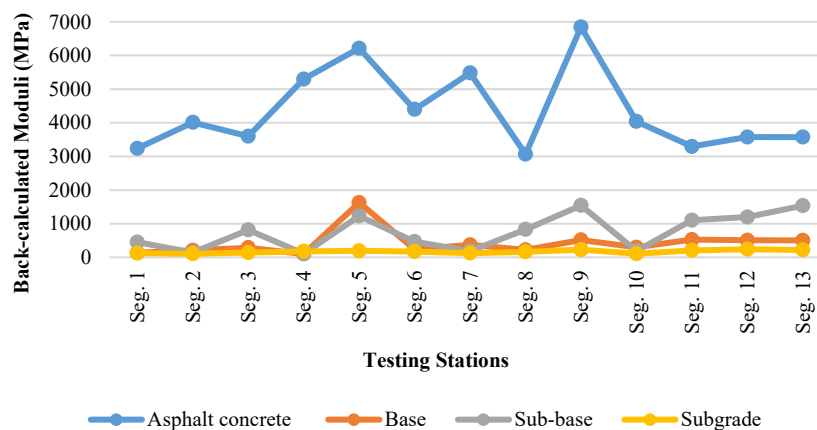


Figure 5. Back-calculated moduli for each layer of the tested segments.

Figure 6a to 6d display the box plot graphs where the descriptive statistics of the back-calculated elastic moduli values can be analyzed for the asphalt concrete layer, base layer, subbase layer, and subgrade, respectively, for the two tested pavement structures (cobblestone interlayer pavement and conventional pavement).

Analyzing the graph of Figure 6a confirms that the asphalt concrete layer of the cobblestone interlayer pavements presented an average moduli of 4740.15 MPa (with a standard deviation equal to 2691 MPa) and the conventional pavements displayed an average moduli equal to 3487.50 MPa (with a standard deviation equal to 1476 MPa). However, the conventional pavement was expected to present higher moduli values due to lower deflection values when tested with the FWD. It also presented lower values of SCI (indicating the better structural performance of the asphalt concrete layer). The variation of coefficient for the cobblestone interlayer pavements was 57%, while it was 42% for conventional pavements, with a minimum value equal to 2010 MPa and a maximum equal to 8804 MPa. This denotes the bigger homogeneity of back-calculated moduli of the asphalt concrete layer of the conventional pavement. Chen et al. (2014), when they performed the structural evaluation on stone interlayer pavement in Louisiana-USA, they also found higher values of moduli for the asphalt concrete layer in this type of pavement compared to those of control pavement made from a stabilized soil-cement base layer. The authors obtained that the average moduli value of the asphalt concrete layer was equal to 5088 MPa for stone interlayer pavement, a value similar to the value obtained in this study.

Figure 6b confirms the cobblestone base layer presented an average moduli of 436 MPa (with a standard deviation equal to 709 MPa and CV equal to 163%) and a granular base layer presented an average moduli equal to 512.78 MPa (with a standard deviation equal to 394 MPa and CV equal to 77%). Chen et al. (2014) obtained an average value of the stone base layer back-calculated moduli equal to 305 MPa when testing the stone interlayer of highway LA-97 in Louisiana-USA. These

authors also tested seven other roadways in Louisiana built with stone base layers. The average values found in the back-calculated moduli for these layers varied from 297 MPa to 619 MPa.

One can confirm that the BDI values on the graph in Figure 4 extrapolated the limit value in the segments with cobblestone base layer. The segments with granular base layer achieved better performance in dissipating tensions and deformation for the lower layers (presented lower values of BDI when compared with the limit value).

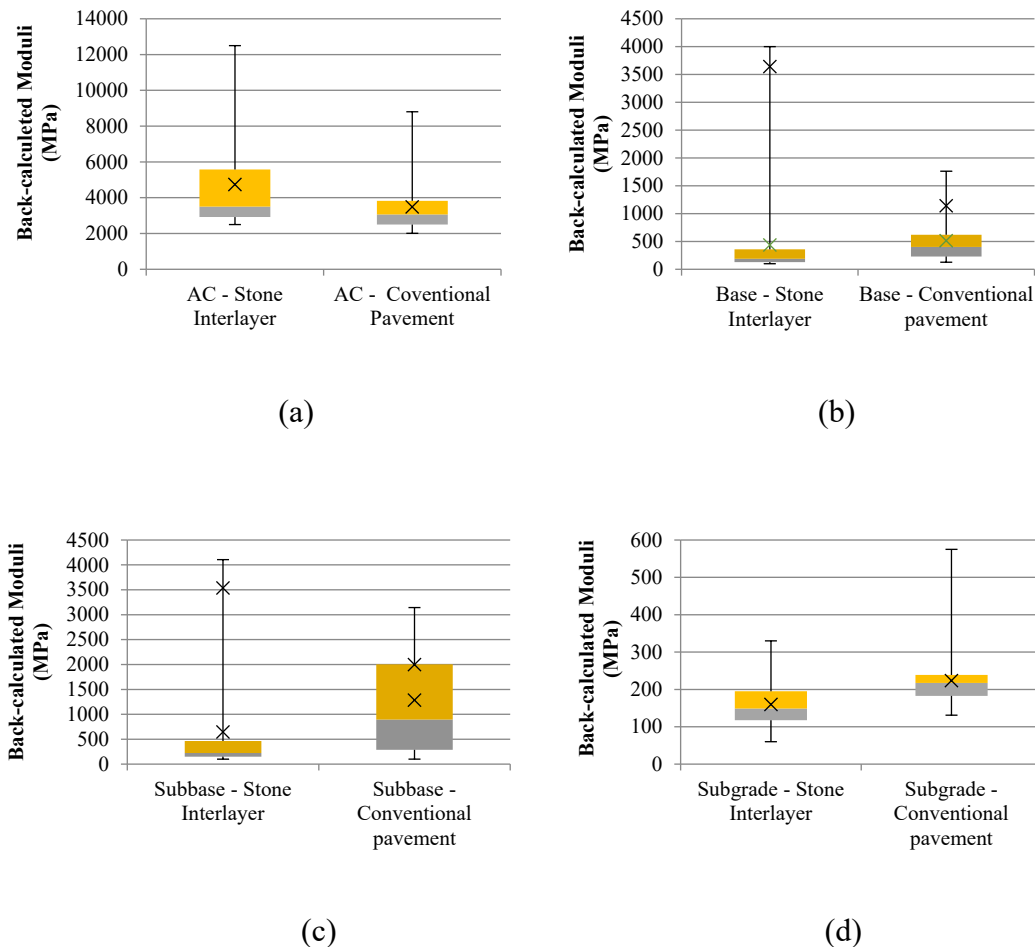


**Figure 6.** Descriptive statistics of the back-calculated moduli values for: (a) the asphalt concrete layer; (b) base layer; (c) subbase layer; (d) subgrade.

By looking at the moduli values of the pavement subbase layer presented in Figure 6c, the bigger stiffness was verified in the conventional pavements (1284.65 MPa) compared to the cobblestone interlayer pavements (643.46 MPa). One explanation for decreased stiffness of the subbase layer in the cobblestone pavement interlayer is that it is made from sand bedding. In contrast, the conventional pavement is made from a well-compacted granular material.

As show in Figure 6d, the average value of the subgrade layer moduli was less than 159.42 MPa while the average value of the same layer of conventional pavement was 223.53 MPa. Chen et al. (2014) achieved the back-calculated average moduli of the subgrade layer from the cobblestone interlayer pavement equal to 184 MPa.

The BCI parameter values of the subgrade layer of conventional pavements are more homogenous and lower than the values of subgrade layer of cobblestone interlayer pavements, as shown in graph 4. The lower BCI values indicate an improved structural condition of the subgrade layer.

In the conventional pavements of this study, the base and subbase layers are made from granular materials from larger moduli, playing an essential role in distributing tensions in the structure of the pavement and relieving the pressure of applied vehicle loads in the subgrade layer.

#### 4.4. Fatigue cracking prediction

The mechanistic-empirical analysis to predict the fatigue cracking in the 13 segments was performed employing the back-calculated moduli averages for each layer of that tested segments. Cracked area (CA) results for each tested segment and the  $N_{AASHTO}$  to achieve 30% of the cracked area for each tested segment are presented in Table 3.

**Table 3:** Cracked area results for each tested segment and  $N_{AASHTO}$  to achieve 30% of the cracked area.

| Segments | CA (%)<br>$N = 10^5$ | CA (%)<br>$N = 5 \times 10^5$ | CA (%)<br>$N = 2 \times 10^6$ | CA (%)<br>$N = 2 \times 10^7$ | CA (%)<br>$N = 5 \times 10^7$ | $N_{AASHTO}$ |
|----------|----------------------|-------------------------------|-------------------------------|-------------------------------|-------------------------------|--------------|
| Seg. 1   | 2.40                 | 6.00                          | 26.90                         | 99.00                         | 99.00                         | 2.15E+06     |
| Seg. 2   | 2.40                 | 5.70                          | 24.50                         | 99.00                         | 99.00                         | 2.30E+06     |
| Seg. 3   | 2.10                 | 4.50                          | 15.40                         | 99.00                         | 99.00                         | 3.25E+06     |
| Seg. 4   | 2.30                 | 5.40                          | 22.30                         | 99.00                         | 99.00                         | 2.45E+06     |
| Seg. 5   | 1.40                 | 2.60                          | 5.70                          | 85.80                         | 99.00                         | 9.30E+06     |
| Seg. 6   | 2.10                 | 4.50                          | 15.40                         | 99.00                         | 99.00                         | 3.25E+06     |
| Seg. 7   | 2.00                 | 4.30                          | 14.20                         | 99.00                         | 99.00                         | 3.45E+06     |
| Seg. 8   | 2.20                 | 5.00                          | 19.10                         | 99.00                         | 99.00                         | 2.75E+06     |
| Seg. 9   | 1.50                 | 3.00                          | 7.20                          | 99.00                         | 99.00                         | 6.79E+06     |
| Seg. 10  | 2.20                 | 5.10                          | 19.90                         | 99.00                         | 99.00                         | 2.66E+06     |
| Seg. 11  | 1.80                 | 3.70                          | 10.60                         | 99.00                         | 99.00                         | 4.50E+06     |
| Seg. 12  | 1.80                 | 3.60                          | 10.00                         | 99.00                         | 99.00                         | 4.75E+06     |
| Seg. 13  | 1.70                 | 3.60                          | 9.80                          | 99.00                         | 99.00                         | 4.87E+06     |

All the tested pavements confirmed fatigue cracking rupture when “heavy” and “very heavy” traffic was considered, yet in all the other (“light,” “average,” and “medium heavy”) traffic; all the segments achieved cracked area percentages lower than 30% at the end of the 10-year project period. One can also confirm that conventional pavements present lower values of cracked area when compared to cobblestone interlayer pavements in “light,” “medium,” or “medium heavy” traffic loading. Analyzing the traffic loading by  $N_{AASHTO}$ , it was confirmed that conventional pavements supported higher values until rupturing, followed by segments 9 and 5 made from cobblestone base layer. One can notice that the segments 9 and 5 achieved lower values in the BDI, BCI, and SCI parameters. Thus, indicating good structural conditions. Rahman and Vargas-Nordbeck (2021) assessed the structural performance of pavements treated with thin asphalt concrete overlay as a conservation technique. To accomplish this purpose, FWD and field performance data from six full-scale thin asphalt concrete overlay test sections and a control section with high cracking were collected and analyzed over a period of nearly 8 years. The results indicated that the sections with lower DBI and BCI values presented lower cracking. The authors confirmed that the cracking field measurements presented a good correlation with these parameters, indicating that the sections with higher BDI and BCI values presented more cracking than the other sections.

Lower deflection values were noticed in segments 5, 9, 11, 12, and 13 (Figure 3), which presented better performance related to fatigue cracking. This result agrees with the Fu et al. (2022a) study, which developed a three-dimensional model of finite elements to simulate the cracking variations in pavements without defects and with cracks based on deflection FWD data. The authors stated that deflections on pavements without defects were much fewer than in cracked pavements. Fu et al. (2022b) confirmed that longitudinal cracking on semi-rigid pavements was more noticed in those structures with weaker subgrades. In this study, the conventional pavement presented greater back-calculated average moduli in the subgrade layer (Figure 6c) and better BCI parameters (Figure 4), indicating better structural conditions of this layer compared to the subgrade layer of cobblestone interlayer pavement.

Table 4 presents the average results of the overall cracked area of stone interlayer pavement segments and conventional pavement segments. The average  $N_{AASHTO}$  which caused the stone interlayer pavement to fatigue rupture was equal to  $3.84 \times 10^6$  and  $4.71 \times 10^6$  for conventional pavement. The conventional pavements obtained the  $N_{AASHTO}$  value of 22.65% greater compared to the stone interlayer pavements, showing that the structural performance of well-compacted granular layers is better.

**Table 4:** Average results of the cracked area, including all the stone interlayer pavement segments and the conventional pavement segments.

|             | $N = 10^5$ | $N = 5 \times 10^5$ | $N = 2 \times 10^6$ | $N = 2 \times 10^7$ | $N = 5 \times 10^7$ | $N_{AASHTO}$ to affect<br>30% of the<br>cracked area |
|-------------|------------|---------------------|---------------------|---------------------|---------------------|--|
| cooblestone | 2.06       | 4.61                | 17.06               | 97.68               | 99.00               | 3.84E+06   |
| Granular    | 1.77       | 3.63                | 10.13               | 99.00               | 99.00               | 4.71E+06   |

The stone interlayer pavements presented a better performance in the studies by Rasoulia et al. (2020) and Titi et al. (2003) related to cracking due to fatigue craking when submitted to traffic loading when compared with conventional pavements. In the Titi et al. (2003) study, the stone interlayer pavement received four times more traffic loading before rupturing that the conventional pavement. In the Rasoulia et al. (2020) study, this type of pavement structure presented a life prediction five times greater than conventional pavement based on the traffic loading. Although, there is a constructive difference between stone interlayer pavement structures evaluated in the studies by these authors as that related to the stone interlayer pavement structure evaluated in this study. The stone base layer was overlaid on a stabilized soil-cement layer in Titi et al. (2003) and Rasoulia et al. (2020) studies, providing increased stiffness to the pavement structure. In case of this study, as the cooblestone base layer is overlaid on a sand layer, the pavement structure provides decreased structural performance compared to pavement structures constructed over properly well-compacted granular layers, as in the case of the conventional pavement evaluated here.

## 5. CONCLUSION

This study evaluated the back-calculated moduli of the cobblestone interlayer pavements and the traffic loading capacity of this type of pavement related to the fatigue rupture criterion based on a mechanistic-empirical analysis. The following are the main conclusions of the study:

- Cobblestone interlayer pavements present greater deflection values measured on the FWD tests at the load application point when compared to those measured on conventional pavements



- with unbound granular base layer, indicating that conventional pavements displayed more stiffness;
- The deflection basin parameters obtained from conventional pavements were more homogeneous and closer to the reference values than those pavements obtained from cobblestone interlayer pavements;
  - The backcalculated moduli of the asphalt concrete layer, base and remaining pavement structure presented an overall good agreement with the DBP evaluated. The majority of the SCI parameters of the cobblestone interlayer pavements extrapolate the reference value, indicating that the asphalt concrete layer is more deformable for this type of pavement when compared with conventional pavements;
  - The majority of the BDI parameters of the cobblestone interlayer pavements extrapolated the reference value result, showing worse structural conditions of the base layer of this type of pavement;
  - The lowest stiffness of the subbase layer is attributed to the cobblestone interlayer pavement, it is made from sand, while the conventional pavement is made from properly well-compacted granular material, providing the higher back-calculated moduli;
  - The lower BCI values of the conventional pavement have indicated better subgrade structural conditions, which can be proven by the higher subgrade moduli values;
  - The DBP-based method by FWD test were able to identify the differences between the base layers and the cracking evolution in the flexible pavement segments evaluated. In this regard, related to the traffic loading capacity of the tested pavements on the fatigue rupture criterion, the conventional pavement presented lower values of cracked area compared to the stone interlayer pavement for “light,” “medium,” or “medium heavy” traffic. Analyzing the  $N_{AASHTO}$  that each segment would bear until reaching its rupture limit, it was confirmed that the conventional pavements would bear higher values.
  - The conventional pavements obtained the  $N_{AASHTO}$  value of 22.65% greater than the stone interlayer pavements, showing that the structural performance of well-compacted granular layers is better.

This study contributed to the structural evaluation of pavements built based on cobblestones converted into traditional flexible pavements. The use of DBP can improve the backcalculation process as well as the road management process, enhancing the evaluation of pavement structural conditions. The need to evaluate the stone layer’s impact on the structural condition of this type of structure in the pavement mechanistic-empirical (ME) design was demonstrated.

## REFERENCES

- AASHTO (2015) *Mechanistic-empirical Pavement Design Guide: a Manual of Practice*. 2nd ed. Washington, D.C.: AASHTO.
- Andrade, L.R.; I.S. Bessa; K.L. Vasconcelos et al. (2024) Structural performance using deflection basin parameters of asphalt pavements with different base materials under heavy traffic. *International Journal of Pavement Research and Technology*, v. 17, n. 5, p. 1353-1366. DOI: 10.1007/s42947-023-00307-w.
- Autelitano, F.; E. Garilli and F. Giuliani (2020) Criteria for the selection and design of joints for street pavements in natural stone. *Construction & Building Materials*, v. 259, n. 6, p. 119722. DOI: 10.1016/j.conbuildmat.2020.119722.
- Babadopulos, L.; J.B. Soares and V.T.F. Castelo Branco et al. (2015) Interpreting fatigue tests in hot mix asphalt (HMA) using concepts from viscoelasticity and damage mechanics. *Transportes*, v. 23, n. 2, p. 85-94. DOI: 10.14295/transportes.v23i2.898.

- Camacho-Garita, E.; R. Puello-Bolaño; P. Laurent-Matamoros et al. (2019) Structural analysis for APT sections based on deflection parameters. *Transportation Research Record: Journal of the Transportation Research Board*, v. 2673, n. 3, p. 313-322. DOI: 10.1177/0361198119828284.
- Cao, W.; L.N. Mohammad and P. Barghabany (2018) Use of viscoelastic continuum damage theory to correlate fatigue resistance of asphalt binders and mixtures. *International Journal of Geomechanics*, v. 18, n. 11, p. 04018151. DOI: 10.1061/(ASCE)GM.1943-5622.0001306.
- Chen, C.; S. Lin; R.C. Williams et al. (2018) Non-destructive modulus testing and performance evaluation for asphalt pavement reflective cracking mitigation treatments. *The Baltic Journal of Road and Bridge Engineering*, v. 13, n. 1, p. 46-53. DOI: 10.3846/bjrbe.2018.392.
- Chen, X.; Z. Zhang and J. Lambert (2014) Field performance evaluation of stone interlayer pavement in Louisiana. *The International Journal of Pavement Engineering*, v. 15, n. 8, p. 708-717. DOI: 10.1080/10298436.2013.857774.
- Delgadillo, R. and S. Monsalve (2021) Fatigue testing of Chilean asphalt mixtures and data fitting with phenomenological models. *Road Materials and Pavement Design*, v. 22, n. 12, p. 2919-2930. DOI: 10.1080/14680629.2020.1794941.
- DER (2006) *IP-DE-P00/003: Instrução de Projeto de Pavimentação*. São Paulo.
- DNER-PRO 273 (1996) *Determinação de Deflexões Utilizando Deflectômetro de Impacto Tipo "Falling Weight Deflectometer (FWD)": Procedimento*. Rio de Janeiro.
- El-Ashwah, A.S.; S.M. El-Badawy and A.R. Gabr (2021) A simplified mechanistic-empirical flexible pavement design method for moderate to hot climate regions. *Sustainability*, v. 13, n. 19, p. 10760. DOI: 10.3390/su131910760.
- Franco, F. (2007) *Método de Dimensionamento Mecânico-Empírico de Pavimentos Asfálticos – SISPAV*. Tese (doutorado). Universidade Federal do Rio de Janeiro. Rio de Janeiro.
- Franco, F., L. Motta (2018) *Guia para Utilização de Método Mecânico-empírico: Apresentação dos Programas Desenvolvidos. Relatório parcial IV(A). Convênio UFRJ/DNIT. Projeto DNIT TED N°682/2014*. Brasília.
- Fritzen, M. et al. (2019) Atualização da função de transferência do dano de fadiga para a área trincado do Programa Medina. In *9º Congresso Rodoviário Português*. Lisboa: Centro Rodoviário Português.
- Fu, G.; Y. Zhao; G. Wang et al. (2022a) Evaluation of the effects of transverse cracking on the falling weight deflectometer data of asphalt pavements. *The International Journal of Pavement Engineering*, v. 23, n. 9, p. 3198-3211. DOI: 10.1080/10298436.2021.1886295.
- Fu, G.H.; H. Wang; Y. Zhao et al. (2022b) Non-destructive evaluation of longitudinal cracking in semi-rigid asphalt pavements using FWD deflection data. *Structural Control and Health Monitoring*, v. 29, n. 10, p. ve3050. DOI: 10.1002/stc.3050.
- Garilli, E.; F. Autelitano; R. Roncella et al. (2020) The influence of laying patterns on the behaviour of historic stone pavements subjected to horizontal loads. *Construction & Building Materials*, v. 258, p. 119657. DOI: 10.1016/j.conbuildmat.2020.119657.
- Gong, H.; B. Huang; X. Shu et al. (2017) Local calibration of the fatigue cracking models in the mechanistic-empirical pavement design guide for Tennessee. *Road Materials and Pavement Design*, v. 18, n. sup3, p. 130-138. DOI: 10.1080/14680629.2017.1329868.
- Horak, E. (2008) Benchmarking the structural condition of flexible pavements with deflection bowl parameters. *Journal of the South African Institution of Civil Engineers*, v. 50, p. 2-9.
- IP-02 (2004). *Classificação das Vias*. São Paulo: Secretaria de Infraestrutura Urbana.
- Ishaq, M.A. and F. Giustozzi (2021) Correlation between rheological fatigue tests on bitumen and various cracking tests on asphalt mixtures. *Materials*, v. 14, n. 24, p. 7839. DOI: 10.3390/ma14247839.
- Jiang, X.; J. Gabrielson; B. Huang et al. (2020) Evaluation of inverted pavement by structural condition indicators from falling weight deflectometer. *Construction & Building Materials*, v. 319, p. 125991. DOI: 10.1016/j.conbuildmat.2021.125991.
- Kheradmandi, N. and A. Modarres (2018) Precision of back-calculation analysis and independent parameters-based models in estimating the pavement layers modulus: field and experimental study. *Construction & Building Materials*, v. 171, p. 598-610. DOI: 10.1016/j.conbuildmat.2018.03.211.
- Klug, A.; A. Ng and A. Faxina (2022) Application of the viscoelastic continuum damage theory to study the fatigue performance of asphalt mixtures: a literature review. *Sustainability*, v. 14, n. 9, p. 4973. DOI: 10.3390/su14094973.
- Mabrouk, G.; O.S. Elbagalati; S. Dessouky et al. (2020) Using ANN modeling for pavement layer moduli backcalculation as a function of traffic speed deflections. *Construction & Building Materials*, v. 315, p. 125736. DOI: 10.1016/j.conbuildmat.2021.125736.
- Nery, C.C.Z. and A.G. Santos (2021) Structural evaluation of pavements applying the MeDiNa Method and FWD and Benkelman beam deflection measurements. *Transportes*, v. 29, n. 4, p. 1-14. DOI: 10.14295/transportes.v29i4.2502.
- Norouzi, Y.; S.H. Ghasemi; A.S. Nowak et al. (2022) Performance-based design of asphalt pavements concerning the reliability analysis. *Construction & Building Materials*, v. 332, p. 127393. DOI: 10.1016/j.conbuildmat.2022.127393.
- Oteki, D.A.; A. Yeneneh; D.S. Gedafa et al. (2024) Evaluating the fatigue-cracking resistance of North Dakota's asphalt mixtures. *Transportation Research Record: Journal of the Transportation Research Board*. In press. DOI: 10.1177/03611981241236796.
- Pais, J.; C. Santos; P. Pereira et al. (2020) The adjustment of pavement deflections due to temperature variations. *The International Journal of Pavement Engineering*, v. 21, n. 13, p. 1585-1594. DOI: 10.1080/10298436.2018.1557334.
- Qian, G.; C. Shi; H. Yu et al. (2021) Evaluation of different modulus input on the mechanical responses of asphalt pavement based on field measurements. *Construction & Building Materials*, v. 312, p. 125299. DOI: 10.1016/j.conbuildmat.2021.125299.

- Rahman, M. and A. Vargas-Nordbeck (2021) Structural performance of sections treated with thin overlays for pavement preservation. *Transportation Research Record: Journal of the Transportation Research Board*, v. 2675, n. 8, p. 382-393. DOI: 10.1177/0361198121997816.
- Rasoulia, M.; B. Becnel and G. Keel (2020) Stone interlayer pavement design. *Transportation Research Record: Journal of the Transportation Research Board*, v. 1709, n. 1, p. 60-68. DOI: 10.3141/1709-08.
- Rocha, M.L. (2020) *Influência dos Módulos de Resiliência Iniciais no Procedimento de Retroanálise de Pavimentos Flexíveis*. Dissertação (mestrado). Universidade Federal de Juiz de Fora. Juiz de Fora, MG.
- Saboo, N.; B. Das and P. Kumar (2016) New phenomenological approach for modelling fatigue life of asphalt mixes, *Construction & Building Materials*, v. 121, p. 134-42. DOI: 10.1016/j.conbuildmat.2016.05.147.
- Sabouri, M. and Y. Kim (2014) Development of a failure criterion for asphalt mixtures under different modes of fatigue loading. *Transportation Research Record: Journal of the Transportation Research Board*, v. 2447, n. 1, p. 117-125. DOI: 10.3141/2447-13.
- Sangghaleh, A.E.; E. Pan; R. Green et al. (2014) Backcalculation of pavement layer elastic modulus and thickness with measurement errors. *The International Journal of Pavement Engineering*, v. 15, n. 6, p. 521-531. DOI: 10.1080/10298436.2013.786078.
- Scimemi, F.; G.T. Turetta and C. Celauro (2016) Backcalculation of airport pavement moduli and thickness using the Lévy Ant Colony Optimization Algorithm. *Construction & Building Materials*, v. 119, p. 288-295. DOI: 10.1016/j.conbuildmat.2016.05.072.
- Singh, A.; A. Sharma and T. Chopra (2020) Analysis of the flexible pavement using falling weight deflectometer for Indian National Highway Road Network. *Transportation Research Procedia*, v. 48, p. 3969-3979. DOI: 10.1016/j.trpro.2020.08.024.
- Souza Jr., J.G.D. (2018) *Aplicação do Novo Método de Dimensionamento de Pavimentos Asfálticos a Trechos de Uma Rodovia Federal*. Dissertação (mestrado). Universidade Federal do Rio de Janeiro. Rio de Janeiro, RJ.
- Titi, H.; M. Rasoulia; M. Martinez et al. (2003) Long-term performance of stone interlayer pavement. *Journal of Transportation Engineering*, v. 129, n. 2, p. 118-126. DOI: 10.1061/(ASCE)0733-947X(2003)129:2(118).
- Underwood, S.; C. Baek and Y. Kim (2012) Simplified viscoelastic continuum damage model as platform for asphalt concrete fatigue analysis. *Transportation Research Record: Journal of the Transportation Research Board*, v. 2296, n. 1, p. 36-45. DOI: 10.3141/2296-04.
- Wang, H.; Z. Yang; S. Zhan et al. (2018) Fatigue performance and model of polyacrylonitrile fiber reinforced asphalt mixture. *Applied Sciences*, v. 8, n. 10, p. 1818. DOI: 10.3390/app8101818.
- Wang, R. and X. An (2024) An optimized fatigue model of asphalt binder combining nonlinear viscoelastic and intrinsic healing characteristics. *Construction & Building Materials*, v. 424, p. 135946. DOI: 10.1016/j.conbuildmat.2024.135946.
- Wang, Y.; S. Underwood and Y. Kim (2020) Development of a fatigue index parameter, S<sub>app</sub>, for asphalt mixes using viscoelastic continuum damage theory. *The International Journal of Pavement Engineering*, v. 23, n. 2, p. 1-15. DOI: 10.1080/10298436.2020.1751844.
- Yang, S.; H. Park and C. Baek (2023) Fatigue cracking characteristics of asphalt pavement structure under aging and moisture damage. *Sustainability*, v. 15, n. 6, p. 4815. DOI: 10.3390/su15064815.
- Zhang, Y.; J. Zhang; T. Ma et al. (2023) Predicting asphalt mixture fatigue life via four-point bending tests based on viscoelastic continuum damage mechanics. *Case Studies in Construction Materials*, v. 19, e02671. DOI: 10.1016/j.cscm.2023.e02671.
- Zhao, J. and H. Wang (2021) Mechanistic-empirical analysis of asphalt pavement fatigue cracking under vehicular dynamic loads. *Construction & Building Materials*, v. 284, p. 122877. DOI: 10.1016/j.conbuildmat.2021.122877.